Characterization of A Novel Avalanche Photodiode for Single Photon Detection in VIS-NIR range

M. Stipčević,[1,*] H. Skenderović,[2] and D. Gracin[1]

[1]*Rudjer Bošković Institute, Bijenička 54, P.O.B. 180, HR-10002 Zagreb, Croatia*
[2]*Institute of Physics, Bijenička 46, HR-10002 Zagreb, Croatia*

In this work we investigate operation in the Geiger mode of the new single photon avalanche photo diode (SPAD) SAP500 manufactured by Laser Components. This SPAD is sensitive in the range 400-1000nm and has a conventional reach-through structure which ensures good quantum efficiency at the long end of the spectrum. By use of passive and active quenching schemes we investigate detection efficiency, timing jitter, dark counts, afterpulsing, gain and other important parameters and compare them to the "standard" low noise SPAD C30902SH from Perkin Elmer. We conclude that SAP500 offers an unmatched combination of low noise, excellent timing and thermal stability.

KEYWORDS: APD, detector, entanglement, photon, quantum information, SPAD

PACS numbers: 42.50.Ar,82.80.Kq,85.60.Dw

Introduction

Experiments in quantum information and communication are mostly concentrated on studying photonic state manipulation at the quantum level. This is because photons, among all elementary particles, have unique properties of being easily produced in abundance, easily manipulated, easily transmitted to large distances and yet being relatively easy to detect. At a current state of the art main tools in research an application of quantum information and communication, namely fiber optic light guides and new ultra-bright sources of entangled photons based on parametric downconversion in nonlinear crystals operate in the near infrared range of 700-1550nm [1–6].

Photomultipliers, as traditional photon detectors, have very small quantum efficiency and a large noise in that wavelength range. The next most mature technology of detecting single photons is based upon avalanche photo diodes (APD) [7]. Not all APDs are suitable for that task. Special semiconductor structures, so called SPAD (Single Photon Avalanche Diode), exhibit characteristics required for single photon detection. In principle, silicon and GaAS SPADs offer excellent quantum efficiency, high gain, mechanical robustness, possibility of miniaturization, low power consumption and relatively low cost.

Since early 1980's practically the only APD suitable for single photon detection in visible to near infrared range (400-1000nm) was the C30902SH from PerkinElmer. Single photon sensitivity is reached in the Geiger mode where a single photoelectron may trigger an avalanche pulse of about 10^8 carriers. In this work we have tested a brand new SPAD SAP500 from Laser Components and compared it to performance of the "standard" C30902SH, in the Geiger mode. Both photodiodes utilize the reach-through type of structure, have the same photo sensitive diameter of 0.5mm and similar spectral sensitivity range. Nevertheless, as will be shown, SAP500 shows better overall performance and can therefore be used as an upgrade or a preferred choice for new designs.

In most of the tests performed in this work we have used one C30902SH sample and one SAP500 sample. Additional two samples of SAP500 (denoted SAP500#1 and SAP500#2) with different active area thicknesses and corresponding breakdown voltages were also available for some tests.

Quenching circuits

Single photon detection by an APD assumes reverse bias voltage V_R greater than the "Geiger" or "breakdown" voltage V_{BR}. We define "overvoltage" as $V_{over} = V_R - V_{BR}$.

In order to fully assess characteristics of APD's in Geiger mode one must use some kind of a quenching circuit. In most measurements we have used a simple (but effective !) passive quenching (PQ) circuit shown in Fig. 1(a), optionally followed by a home-made constant level discriminator (CLD) and a 12ns pulse shaper as shown Fig. 1(b). A threshold level of the CLD is fixef at 22.5mV. Due to the capacitive coupling, the circuit in Fig. 1(b) can measure avalanches up to over 2MHz and is highly immune to paralyzation effect [11]. If the current limiting resistor R_S is chosen sufficiently large, an avalanche will cease (quench) by itself within a

*Electronic address: Mario.Stipcevic@irb.hr

sub-nanosecond time. A condition for successful quench is that V_{over}/R_S is smaller than the *latch current* of the given SPAD. At the same time the voltage across the SPAD will drop somewhat below V_{BR}. After the quench, voltage across the diode recovers towards its initial value following the exponential law with the time constant $\tau = R_S C_{SPAD}$, where C_{SPAD} is the capacitance of the reversely polarized SPAD (plus any parasitic capacitances present in the actual circuit). During the bias recovery SPAD operates at lower overvoltages and features photon detection efficiency lower than the nominal.

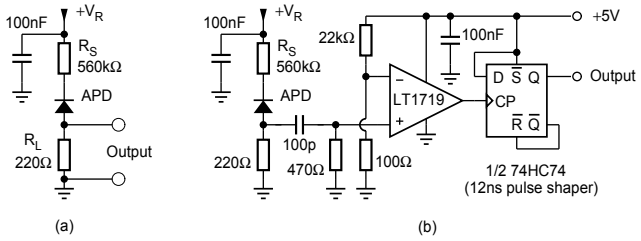

FIG. 1: (a) the passive quenching circuit; (b) the same followed by the constant level discriminator and the pulse shaper.

For those measurements for which the long recovery time of the PQ circuit was prohibitive we have used our previously described active quenching (AQ) circuit [10]. In active quenching, both lowering and restoring of bias voltage are asisted by active electronic components leading to quick recovery and well defined dead time. Neglecting the transition times, in active quenching the SPAD is either completely insensitive to incoming photons or is at its nominal sensitivity. Due to inevitable delays in the electronics, the dead time of an AQ circuit is somewhat longer than the quenching time t_Q during which the SPAD is actually kept below V_{BR}. In our case $t_{dead} \approx t_Q + 20$ns. Slight variations of component values in the circuit allowed us to choose the dead time in the interval of 25-50ns.

Breakdown voltage and its thermal coefficient

When SPAD changes its temperature, a variation in operating voltage is required to maintain the same gain. It has been found empirically [13] that required voltage variation for a reach-through SPAD is a linear function of the operating temperature:

$$V_R(T) = V_R(T_0) + 0.22w(T - T_0) = const. + t_c T \quad (1)$$

where w is the thickness of the active area (depletion region) in μm. Since there is an (approximately linear) relationship between breakdown voltage and the thickness w, the thermal coefficient t_c is also a function of the breakdown voltage. For silicon SPADs thermal coefficient is typically in the range 0.1-0.7V/K. Breakdown voltages and thermal coefficients of the four tested diodes are shown in the Table I. We see that SAP500 features a significantly smaller thermal coefficient than C30902SH which, in conjunction with smaller operating voltage (thus smaller heat production), leads to much better stability of operation, especially in case of strongly varying illumination.

	C30902SH	SAP500#1	SAP500	SAP500#2
V_{BR}@18^{o}C	215.2V	103.7V	118.3V	135.1V
t_c	0.68V/K	0.196V/K	0.27V/K	0.33V/K

TABLE I: Breakdown voltages and thermal coefficients of the tested SPADs.

Multiplication gain and effective capacitance

Figure 2 shows average single photon responses of the two SPADs, as measured by a 10MΩ 8pF oscilloscope probe at the output of the PQ circuit in Fig. 1(a).

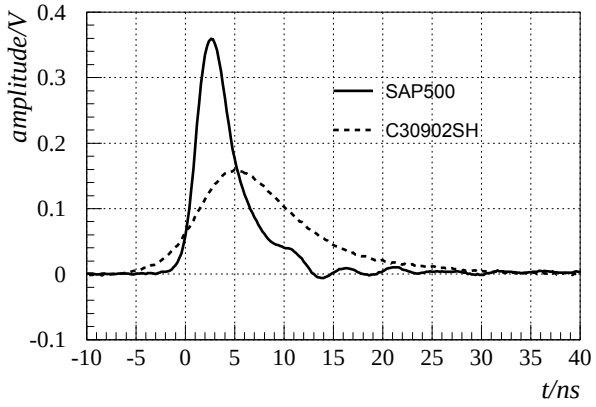

FIG. 2: A single photon response at the output of the passive quenching circuit, for SAP500 and C30902SH. Because of pulse to pulse variations, a statistical average of 256 output waveforms are shown.

the output of the PQ circuit at $V_{over} = 5$V. Multiplication gain G is defined as a number of electrons produced (on average) by a single converted photon:

$$G = \frac{1}{R_L e} \int_0^\infty V(t)dt. \quad (2)$$

where V(t) is the voltage at the output of the PQ circuit. Gain as a function of overvoltage for single photons of 676nm is shown in Fig. 3. Gains of both diodes are of the similar magnitude but due to its much shorter pulse SAP500 produces a higher peak. Interestingly, gain of these tiny devices is up to a couple of hundred times higher than the gain of conventional 10 dynode photo multipliers which is typically on the order of 10^6.

By virtue of charge conservation, the total charge delivered by the avalanche is equal to the product of the

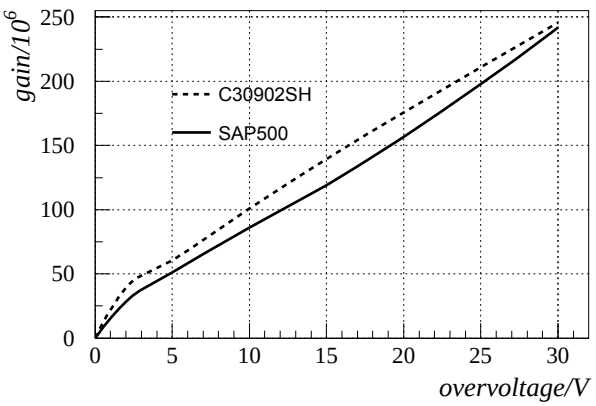

FIG. 3: Multiplicaton gain (in millions) as a function of overvoltage for single photons of 676nm at room temperature.

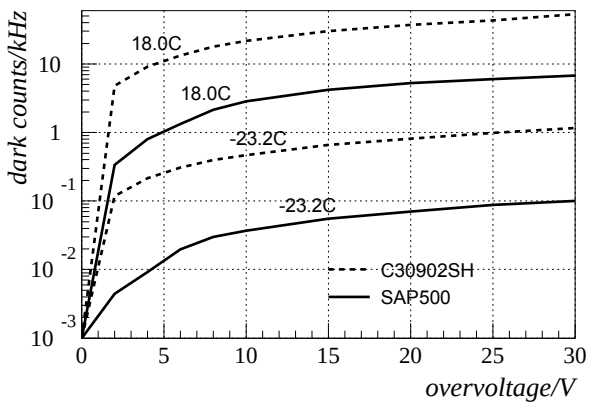

FIG. 4: Dark counts rate as function of overvoltage measured at two temperatures.

SPAD's capacitance (plus any parasitic parallel capacitance) and the voltage step the SPAD makes during the quench. If a capacitance C_p is added in parallel to the SPAD, the charge delivered within one pulse rises by the factor $(C_{SPAD}+C_p)/C_{SPAD}$ where C_{SPAD} includes parasitic capacitance of the PQ circuit which has been estimated to 2pF. Using $C_p = 3.3$pF we obtained capacitances of 1.50pF for C30902SH and 1.63pF for SAP500. Although the two capacitances are very similar, due to the larger avalanche current SAP500 produces narrower and higher pulse with roughly 2.9 times faster rise time (10-90%) than C30902SH (Fig. 2) leading to a much better time resolution, as will be established by direct measurement.

Dark counts

In photon counting technique dark counts present an unwanted noise. The highest tolerable noise in most applications lies between a few hundred Hz and a couple of kHz. For such a low average counting frequency, performance of a SPAD can be assessed quite precisely with the passive quenching circuit. Fig. 4 shows dark counts of C30902SH and SAP500 at 18.0^{o}C and -23.2^{o}C as a function of overvotage.

The C30902SH has already been selected for low noise, whereas SAP500 samples have been randomly chosen from a batch. Here we can draw two conclusions.

First, typical unselected SAP500 SPAD features a lower noise than C30902SH. Notably, the 118.3V sample exhibits less than 100cps dark counts rate for an overvoltage up to 30V at -23.2^{o}C.

Second, cooling from 18.0^{o}C to -23.2^{o}C reduces dark counts rate more for SAP500 than for C30902SH. Reduction factor for C30290SH is about 46 while for SAP500 it is about 75.

Finally, by testing several samples of SAP500, it came to our attention that thicker SPADs (i.e. those with greater V_{BR}) tend to be noisier. This is easy to understand qualitatively since diodes with a thinner active area have smaller volume which can contain impurities responsible for dark counts.

Dead time

As explained above, the dead time, which is equal to the sum of the quenching time t_Q plus delays in the electronics, is a pure feature of the AQ circuit. An oscillogram of the detector's output made of pileup of many detected photons is shown in Fig. 5. It shows gaps between a photon detection and the next detection. The minimum observed gap is then, by definition, the dead time.

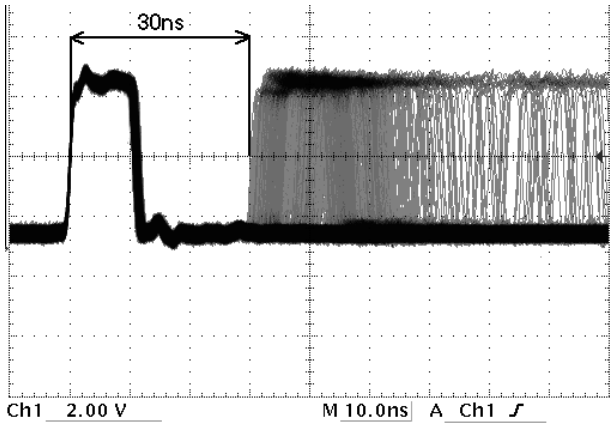

FIG. 5: Pileup of many detected photons. Dead time is the minimum delay observed between any detected photon and the next detected photon.

In a well designed A.Q. circuit one can set the dead time at will, starting from some minimum value determined by the circuit design and speed of the used active electronics components. However, in practical application, the dead time should not be made too small because t_Q alone has to be chosen long enough

to allow for annihilation of carriers created by the avalanche in order to keep the afterpulsing probability at an acceptable level. Here we have two competing effects: dark counts and the dead time. Namely, the half-life of carriers depends on the diode's structure as well as its operating temperature. While low operating temperature is favorable for low noise operation, it causes a longer carrier half-life and thus requires longer t_Q and consequently longer dead time.

This effect is clearly seen in C30902SH where successful quenching with the 12V step and t_Q=20ns (dead time 40ns) is possible up to an overvoltage of 7-7.5V at room temperature, whereas at -23.2^{o}C it is possible to quench only up to 4-4.5V ! To quench at higher overvoltages one must use longer quenching time in order to allow all impurity centers to release trapped carriers. According to the datasheet [9], operating C30902SH at an overvoltage of 25V would require quenching time as long as 300ns ! Such a long quenching time (and corresponding dead time) is unsatisfactory for many applications.

On the other hand, cooling of the available SAP500 samples down to -23.2^{o}C and using t_Q as low as 5ns (dead time 25ns) at overvoltages of up to 10V did not cause any problems with quenching. From this we conclude that SAP500 allows for lower dead time (i.e. better photon pair resolution) than C30902SH.

Afterpulsing probability

Afterpulse in a SPAD is caused by a carrier left over from a previous avalanche, trapped in an impurity and then released at a latter time. If such a carrier makes its way to the avalanche region it may cause an avalanche which is indistinguishable from a true photon detection. Important parameters for afterpulsing probability are impurity concentration and carrier lifetime. In silicon SPADs afterpulsing is a fast process decaying in about few tens to few hundreds nanoseconds therefore the active quenching is necessary in order to capture afterpulses and measure the afterpulsing probability. We define afterpulsing probability (a.p.) as a probability that an afterpulse will appear after a detection of a photon. According to this definition we have constructed a setup for measuring the a.p. as shown in Fig. 6.

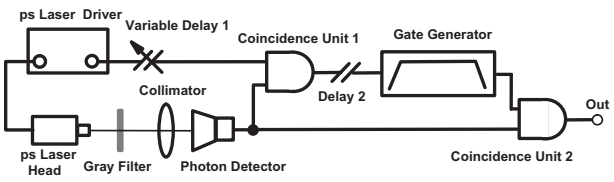

FIG. 6: Setup for measurement of afterpulsing probability.

Ultra short, weak pulses of light from a pulsed laser (PicoQuant PDL 800-D, laser head 39ps FWHM, λ=676nm) are fired into the detector. Pulse energy and gray filter are chosen such that the detector receives almost exclusively either 0 or 1 photon per pulse whereas two and more photon events are strongly suppressed. Delay 1 is adjusted such that in case that a photon has been fired and detected, the Coincidence Unit 1 generates a logic pulse. Due to a short coincidence window (20ns) and low dark counts rate (up to a few kHz) accidental coincidences are negligible. The pulse is delayed for 100ns (Delay 2) after which the Gate Generator opens the gate of the Coincidence Unit 2 for the next 400ns.

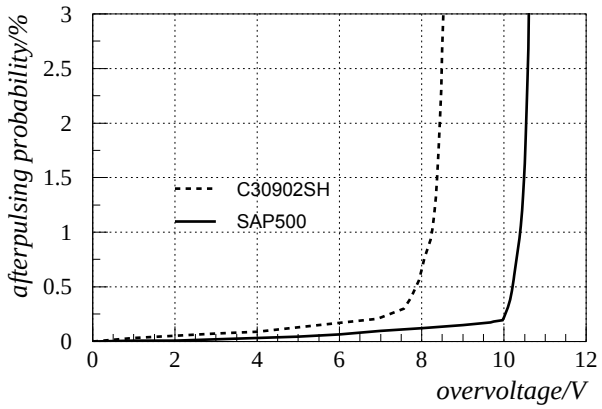

FIG. 7: Afterpulsing probability as a function of overvoltage for the to SPADs, at the temperature of 18^{o}C, measured by active quenching.

In such a way afterpulses generated between 100-th and 500-th nanosecond after the photon detection appear at the output. The afterpulsing probability is then simply given as the ratio of the frequency of afterpulses at the output of the second coincidence unit and the frequency of detected pulses at the output of the first coincidence unit. Measured afterpulsing probabilities as functions of overvoltage are shown in Fig. 7. We see that both diodes perform well up to some critical overvoltage where a.p. rises quickly. The rise is the effect of the active quenching circuit as will be explained in the next section.

Diving voltage

Avalanches in Geiger mode appear at an inverse bias voltage greater than V_{BR}. Successful quenching of such avalanches requires lowering the bias voltage somewhat below V_{BR}, namely to $V_{BR}-V_D$ where V_D is the "diving" voltage. How "deep" the bias voltage must go below the V_{BR} depends on the diode structure, impurities and concentrations of dopands. For most purposes, the best photon counting performance of SPADs is obtained by active quenching. However, since an active quenching circuit can only make a finite (limited) voltage step, SPADs with smaller diving voltage will be able to work at a higher overvoltage and thus, generally, yield a better performance than those with bigger diving voltage.

The diving effect can be observed by passive quenching circuit Fig. **??**(a). The SPAD is illuminated with a constant light flux and the voltage over the R_L is measured by a passive probe. When a photon is detected a waveform is recorded from this pulse (trigger) onwards. Many such waveforms are recorded, stored and overlayed by use of a digital storage oscilloscope (Tektronix TDS3052B). The resulting picture for C302902SH is shown in Fig. 8 (a similar one is obtained with SAP500).

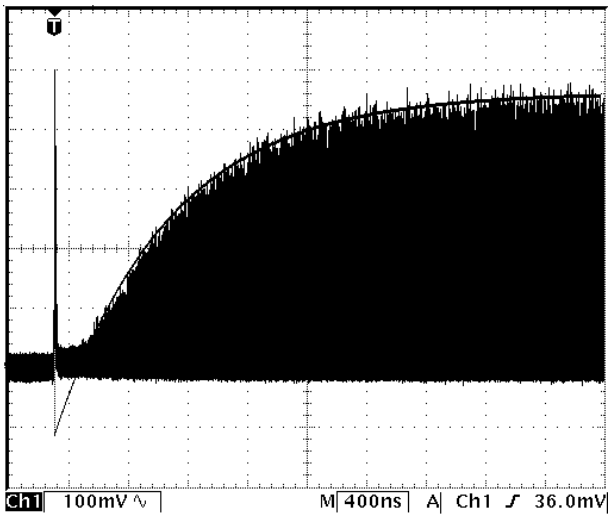

FIG. 8: Illustration of the diving effect for C30902SH, obtained by means of the passive quenching circuit.

Photons detected before full recovery of the bias voltage produce smaller peak (lower gain!). Fitted exponential envelope corresponds to the bias recovery following an avalanche. We can see that after the trigger there is a certain period of time during which no detection is possible. This is because the bias voltage is then below V_{BR} due to the diving effect, as is clearly illustrated by the fitted envelope.

In this section we measure diving voltages of SAP500 and C30902SH by means of the active quenching circuit. With active quenching one can directly measure V_D whereas with passive quenching extraction of the diving voltage is complicated with modeling of the electronics and response of the SPAD. Measuring the V_D with the AQ circuit consists of finding the highest value of overvoltage (critical overvoltage) at which quenching can be done efficiently. Namely, if the voltage step provided by the AQ circuit is not sufficient, there will be an elevated probability of unsuccessful quench after which the AQ circuit will initiate another quenching attempt and so forth until quenching finally succeeds. Looking at the output of the detector, this effect can be seen on the oscilloscope as a series of pulses separated approximately by one dead time (Fig. 9).

Because the additional quenching attempts are counted as afterpulses, the critical overvoltage is characterized by a sharp rise in afterpulsing probability [10] as can be seen in the Fig. 7. The diving voltage is then simply the difference between the voltage step (in our case 12V) and the critical overvoltage. From these graphs we estimate the diving overvoltages of C30902SH to be ≈4-4.5V and of SAP500 ≈2V. We also see that transition from efficient to inefficient quenching regime is much sharper for SAP500 than for C30902SH which offers more stable operation near the critical overvoltage.

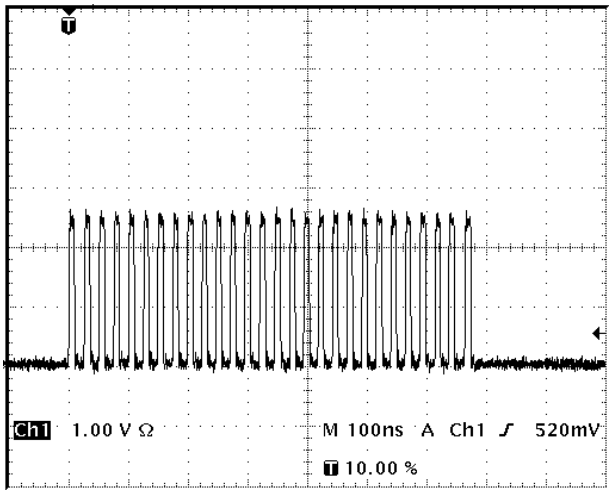

FIG. 9: Inefficient quenching condition at too high an overvoltage - a cascade of quenching attempts.

Time resolution (jitter)

In many experimental methods such as time resolved spectroscopy, quantum communication or range finding, precise timing of photon arrival is essential. Photon arrival time resolution (timing jitter) has been measured by use of the passive quenching circuit with the constant level discriminator shown in Fig. 1(b) and the whole measurement setup is shown in Fig. 10.

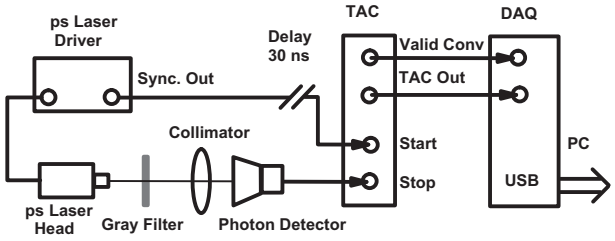

FIG. 10: Setup for measuring timing jitter of a SPAD based photon detector by means of a picosecond laser and time-to-amplitude converter (TAC).

Arrival time is measured with the time-to-amplitude converter (TAC) Ortec model 567 which has a resolution of 10ps. Width of the laser pulse (39ps) and jitter of the electronics (25ps) are negligible in these measure-

ments. The measured jitter is nearly a Gaussian function. For illustration we show the distribution for SAP500 at V_{over} = 30V and $T_{SPAD} = -23.2^oC$ (Fig. 11). A fitted Gaussian is also shown. The right side tail, characteristic of reach-through structure, is barely present.

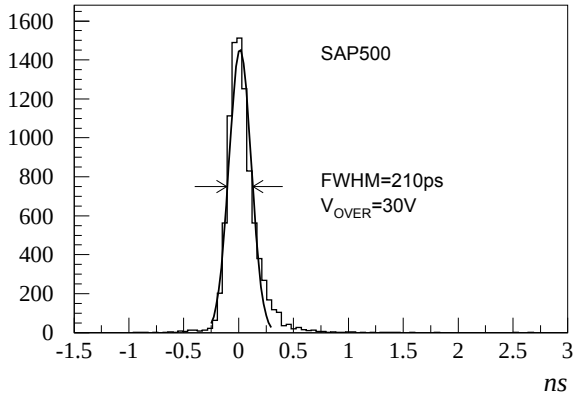

FIG. 11: Near Gaussian jitter distribution for SAP500 at -23.2^{o}C and overvoltage of 30V. The right side tail, charcteristic of reach-through structure, is barely visible.

Jitter as a function of overvoltage is shown in Fig. 12. Measurements have been made at a low temperature (-23.2^{o}C) at which SPADs are normally used. As is well known, SPADs utilizing reach-through structure are not optimal for timing purposes [12]. Nevertheless, we see that SAP500 offers quite good timing resolution (450ps at V_{over}=10V, 210ps at V_{over}=30V), comparable to the best photomultiplier based single photon detectors, even with this simple passive circuit with the CLD. A further improvement of resolution can be expected with use of a constant fraction detection (CFD) principle.

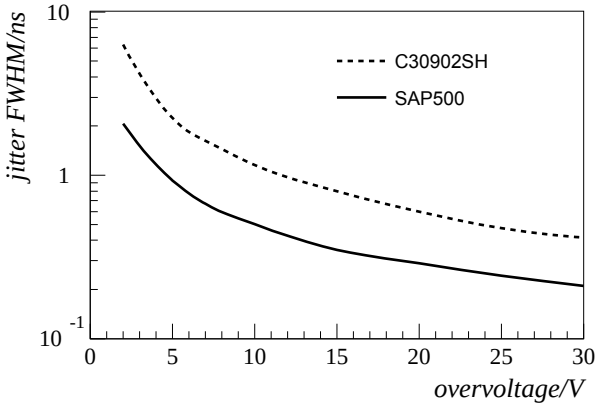

FIG. 12: Timing resolution (jitter) FWHM as a function of overvoltage for the two SPADs, measured with the passive quenching circuit and a constant fraction detector. At overvoltage of 30V jitter goes down to 420ps for C30902SH and 210ps for SAP500.

Absolute detection efficiency at 810nm

Photon detection efficiency (PDE) is defined as the ratio of frequency detected photons and frequency of photons impinging the active surface of the APD. Thanks to the development of the technique of spontaneous parametric downconversion, it is now possible to determine absolute photon detection efficiency of single photon detectors in a relatively simple manner. Our setup, shown in Fig. 13, follows the general idea of [8]. Having prepared the setup, measurement of absolute detection efficiency requires only a small number of measurements and no standards.

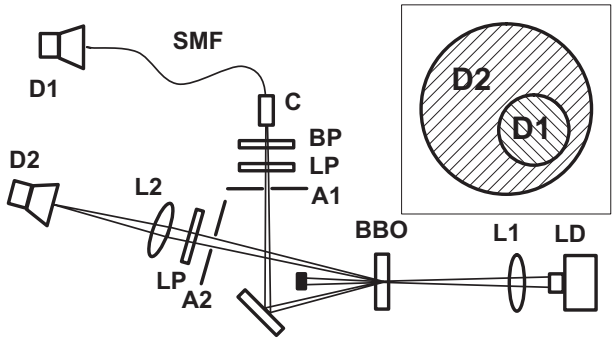

FIG. 13: Setup for measuring absolute detection efficiency at 810nm by use of the type-II parametric downconversion in BBO crystal.

We start with two detectors of unknown efficiencies (D1 and D2) and want to determine efficiency of the D2. A type-II spontaneous parametric downconversion setup, consisting of 405nm laser pump and conveniently cut BBO crystal, produces pairs of photons. Two photons in a pair are emitted almost simultaneously ($\Delta t \sim$100fs) each within a very thin cone. The two cones are tilted $\pm$3 degrees from the direction of the pump. One photon from a pair is directed towards D2. In this arm we want transmission loses to be as small as possible therefore only a longpass filter (Thorlabs FGL715) needed for reducing the laser glow and anti-reflective coated collimating lens are used. The other photon from the pair is directed towards pigtailed detector D1 (PerkinElmer SPCM-AQRH-14).

The crucial consideration is that the detector D1 has a smaller viewing angle than D2 in such a way that if D1 has detected a photon then D2 has surely received (but not necessarily detected) the other photon from the pair. This condition can be achieved by adjustment of apertures A1 and A2. With this in mind one has:

$$F_1 = T_1\epsilon_1^{'} + N_1 \quad (3)$$

$$F_2 = T_2\epsilon_2^{'} + N_2 \quad (4)$$

$$C = T_1\epsilon_1^{'}\epsilon_2^{'} + N_1F_2\tau_c \quad (5)$$

where T_i, F_i, N_i and $\epsilon_i^{'}$ are: true frequency of photons falling on the detector, frequency of detected photons, noise (dark counts) and effective detection efficiency which includes transmission and dead time losses, respectively for the i-th detector. C is the coincidence rate within the time window of τ_c =5.5ns. In our case, the coincidence rate is about 7.5kHz while the term $N_1 F_2 \tau_c$ amounts only 3-4 Hz and is therefore negligible. After elimination of unknown $T_1 \epsilon_1{}'$ from the first and last line we obtain the expression for the efficiency of the detector D1:

$$\epsilon_2 = k\epsilon_2^{'} = k\frac{C}{F_1 - N_1}. \quad (6)$$

where the factor $k \approx 1.10$ accounts for transmission losses in the filter and lens in front of the D2 as well as the dead time correction. While the coated lens has a transmission coefficient of nearly 1, the transmission coefficient of the low-pass filter can be measured quite precisely as a factor of drop of detection rate of D2 when another identical filter is inserted. The filtering in the other arm has no effect to the measurement, except that the bandpass filter (810±5)nm defines the wavelength at which the PDE is measured. Knowing the absolute detection efficiency at 810nm allows us to properly scale the relative spectral efficiency curve (measured below) so that it becomes an absolute one.

Spectral detection efficiency

Relative spectral detection efficiency has been measured with the setup shown in Fig. 14.

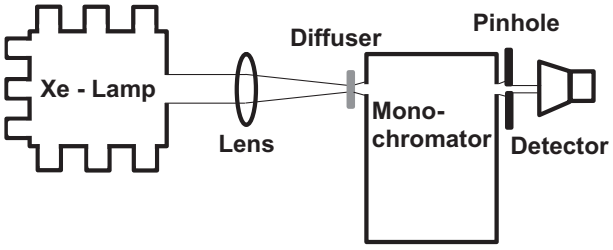

FIG. 14: Setup for measuring relative absolute detection efficiencies at various wavelengths by use of a monochromator.

Power P_{emit} emitted from the output of the monochromator (Spectral Products CM110) at chosen wavelengths is known (calibrated). The detector under test is homogeneously illuminated through a pinhole by a small fraction of the emitted light power, P_{inc}. The photon detection efficiency ϵ at a given wavelength λ is then given by:

$$\epsilon(\lambda) = \frac{f_{det}(\lambda)}{f_{inc}(\lambda)} = \frac{f_{det}(\lambda)}{P_{inc}(\lambda)/(hc/\lambda)} = k\frac{f_{det}(\lambda)}{\lambda P_{emit}(\lambda)}. \quad (7)$$

where f_{det} is frequency of detected photons, f_{inc} is frequency of photons impinging on the detector's sensitive area whereas k is an unknown constant defined by the geometry of the setup. This constant can be determined by a single known value of detection efficiency at some wavelength, for example previously measured $\epsilon(810nm)$:

$$k = \frac{\epsilon(810\text{nm}) \times 810\text{nm} \times P_{emit}(810\text{nm})}{f_{det}(810\text{nm})}. \quad (8)$$

Spectral sensitivity in Geiger mode can only be defined up to an arbitrary multiplicative constant:

$$S(\lambda) \propto \frac{f_{det}(\lambda)}{P_{emit}(\lambda)}. \quad (9)$$

which we choose such that the peak of the curve is at 1. Spectral curves measured for the two SPADs are shown in Fig. 15. The peak PDE of C30902SH is at longer wavelength than the peak of SAP500. This is expected since C30902SH has a thicker active region. On the other hand due to its lower noise and smaller diving voltage, SAP500 can be operated at higher overvoltages thus effectively obtaining better PDE at all wavelengths.

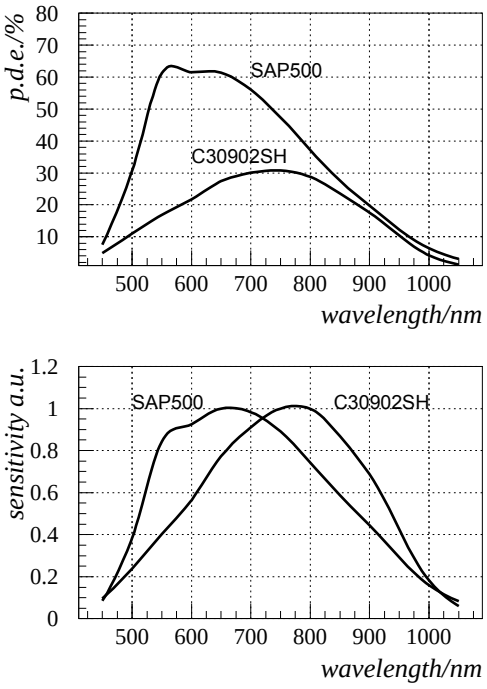

FIG. 15: Spectral photon detection efficiencies and spectral sensitivities for C30902SH at V_{over}=6V and SAP500 at V_{over}=10V.

We can see that peak PDE of SAP500 is between 550nm and 650nm whereas of C30902SH is at approx. 800nm. Nevertheless, due to much better afterpulsing

performance SAP500 can be operated at higher overvoltages thus achieving comparable performance in the NIR and quite significantly better performance in the visible spectrum.

Detection efficiency versus overvoltage

Probably the most important consideration in photon detector design is its detection efficiency which ideally should be as high as possible. In SPADs, photon detection efficiency, at any chosen wavelength, rises with applied overvoltage and asymptotically approaches quantum efficiency.

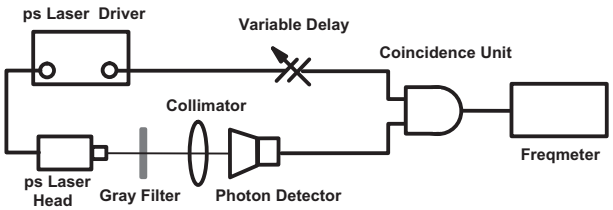

FIG. 16: Setup for measuring photon detection efficiency as a function of the overvoltage by use of the pulsed laser and the coincidence technique.

The measurement was performed using the setup shown in Fig. 16. The picosecond pulsed laser (λ=676nm) is periodically fired in such a way that either 1 or 0 photons reach the SPAD. The coincidence gate is open in synchronization with every emitted photon and thus the frequency meter counts all detected photons while the dark counts are almost completely suppressed due to a very short coincidence window of only 20ns. Furthermore, SPADs were kept at a low temperature (-23.2^{o}C) so that the loss of detection efficiency due to dead time caused by dark pulses is kept at a negligible level. In that conditions, reading at the frequency meter is directly proportional to the photon detection efficiency at 676nm.

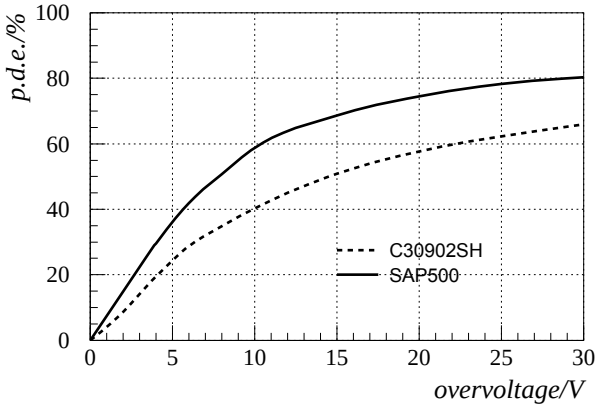

FIG. 17: Photon detection efficiencies as a function of the overvoltage at 676nm. SPADs were kept at -23.2^{o}C.

Knowing the value of p.d.e. at 676nm and at 10V overvoltage (which can be read from the spectral graph in Fig. 15) one can turn these relative efficiencies into absolute ones, which are shown in the Fig. 17. As expected we see that p.d.e. rises with the overvoltage and saturates at some value close to the declared quantum efficiency of each SPAD at the given wavelength. However, as we have seen throughout this paper, the maximum practicaly achievable p.d.e. depends on levels of noise and afterpulses which also rise with the overvoltage.

Conclusion

A new SPAD SAP500 has been evaluated for a single photon detection in the wavelength range of 400-1000nm and compared to the performance of the "standard" C30902SH. SPADs have been operated in the Geiger mode and a wide range of experimental techniques and setups including both passive and active quenching methods was used. We have found that SAP505 shows simultaneously an excellent noise performance (down to 50Hz), low afterpulsing ($<$ 0.25%) and high photon detection efficiency (up to 62% at 650nm) at the overvoltage of 10V. Furthermore, a small value of the breakdown voltage thermal coefficient of typically 0.27V/K and a small bias voltage make operation of SAP500 more stable even in the conditions of rapidly changing count rate. All the above makes SAP500 an interesting upgrade replacement or a preferred choice for SPAD based single photon detection applications in VIS-NIR range.

Ackgnowledgements

This work was supported by project "Photon detector" financed by Croatian Institute of Technology 2007-2010 and by Ministry of science education and sports of Republic of Croatia, contract number 098-0352851-2873.

[1] P. G. Kwiat et al., New High-Intensity Source of Polarization-Entangled Photon Pairs, Phys. Rev. Lett. **75**, 4337-4341 (1995)

[2] P. G. Kwiat et al., Ultra bright source of polarization entangled photons, Phys. Rev. **A 60**, R773R776 (1999)

[3] A. Poppe et al., Practical quantum key distribution with polarization entangled photons Opt. Express **12**, 3865-3871 (2004)

[4] D. Stucki et al., Quantum key distribution over 67 km with a plug&play system, New Journal of Physics 4 (2002) 41.141.8

[5] T. Jennewein, U. Achleitner, G. Weihs, H. Weinfurter, and A. Zeilinger, A fast and compact quantum random number generator, Rev. Sci. Instrum. **71**(2000)16751680.

[6] M. Stipcevic, B. Medved Rogina, Quantum random number generator based on photonic emission in semiconductors, Rev. Sci. Instrum. 78(2007)045104:1-7

[7] H. Dautet et al., "Photon counting techniques with silicon avalanche photodiodes", Appl. Optics **32**(1993)3894-3900

[8] J.G.Rarity, K.D.Ridley, P.R.Tapster, "Absolute measurement of detector quantum efficiency using parametric downconversion", Appl. Optics 26(1987)4616-4619

[9] "Silicon avalanche photodiodes C30902E, C30902S, C30921E, C30921S", (data sheet), EG&G Canada, January 1, 1991

[10] M. Stipčević, Active quenching circuit for single-photon detection with Geiger mode avalanche photodiodes, Appl. Optics 48(2009)1705-1714

[11] K. Schätzel, R. Kalström, B. Stampa, and J. Ahrens, "Correction of detection-system dead-time effects on photon-correlation functions", J. Opt. Soc. Am. B **5**(1989)937-947

[12] S. Cova, M. Ghioni, A. Lotito,I. Rech, and F. Zappa, Evolution and prospects for single-photon avalanche diodes and quenching circuits, J. Mod. Opt. **51** (2004)1267-1288

[13] Laser Components GmbH, Silicon Avalanche Photodiodes, Technical note 08/06/V2/HW, Aug.2006, Web URL: http://www.lasercomponents.com/fileadmin/user_upload/home/Datasheets/lc/applikationsreport/si-apds.pdf